

Electrocorticographic activity over sensorimotor cortex and motor function in awake behaving rats

Chadwick B. Boulay, Xiang Yang Chen, and Jonathan R. Wolpaw

Laboratory of Neural Injury and Repair, Wadsworth Center, New York State Department of Health, Albany, New York; and State University of New York, Albany, New York

Submitted 17 September 2014; accepted in final form 15 January 2015

Boulay CB, Chen XY, Wolpaw JR. Electrocorticographic activity over sensorimotor cortex and motor function in awake behaving rats. *J Neurophysiol* 113: 2232–2241, 2015. First published January 28, 2015; doi:10.1152/jn.00677.2014.—Sensorimotor cortex exerts both short-term and long-term control over the spinal reflex pathways that serve motor behaviors. Better understanding of this control could offer new possibilities for restoring function after central nervous system trauma or disease. We examined the impact of ongoing sensorimotor cortex (SMC) activity on the largely monosynaptic pathway of the H-reflex, the electrical analog of the spinal stretch reflex. In 41 awake adult rats, we measured soleus electromyographic (EMG) activity, the soleus H-reflex, and electrocorticographic activity over the contralateral SMC while rats were producing steady-state soleus EMG activity. Principal component analysis of electrocorticographic frequency spectra before H-reflex elicitation consistently revealed three frequency bands: $\mu\beta$ (5–30 Hz), low γ (γ_1 ; 40–85 Hz), and high γ (γ_2 ; 100–200 Hz). Ongoing (i.e., background) soleus EMG amplitude correlated negatively with $\mu\beta$ power and positively with γ_1 power. In contrast, H-reflex size correlated positively with $\mu\beta$ power and negatively with γ_1 power, but only when background soleus EMG amplitude was included in the linear model. These results support the hypothesis that increased SMC activation (indicated by decrease in $\mu\beta$ power and/or increase in γ_1 power) simultaneously potentiates the H-reflex by exciting spinal motoneurons and suppresses it by decreasing the efficacy of the afferent input. They may help guide the development of new rehabilitation methods and of brain-computer interfaces that use SMC activity as a substitute for lost or impaired motor outputs.

H-reflex; motor control; spinal cord; cortex; brain-computer interface

THE RELATIONSHIPS between cortical activity and motor function have been studied since the original demonstrations of cortical excitability by Fritsch and Hitzig (1870) and Ferrier (1886) in the late 19th century (Gross 2007), and they continue to be a major research focus (Ashe et al. 2006; Graziano et al. 2002; Miller et al. 2012; Rizzolatti and Luppino 2001). These studies are driven by both basic science and clinical interests. As basic science, they offer insight into how the central nervous system (CNS) accomplishes its primary function, to produce appropriate behaviors that serve the needs of the organism. As clinical research, they offer new possibilities for restoring motor function to those afflicted by severe neuromuscular disorders, including strokes, spinal cord injuries, and cerebral palsy.

Among the most surprising and promising outcomes of recent work is the realization that cortical activity exerts long-term as well as short-term control over the simplest

aspects of motor function: the spinal cord reflex pathways that are part of the substrate supporting all motor behaviors. As a result, spinal cord reflexes are serving as models for studying CNS function and plasticity and as therapeutic targets in spinal cord injury, stroke, and other disorders (Chen et al. 2006c; Thompson et al. 2013; Wolpaw 2010).

The H-reflex is a particularly attractive experimental model because it is mediated by a wholly spinal and largely monosynaptic spinal pathway (Henneman et al. 1965; Matthews 1972). The motoneuron excitation produced by the H-reflex pathway contributes to locomotion and to other important behaviors; despite its apparent simplicity, the pathway adapts to the requirements of these different behaviors in the short term (e.g., standing or walking or running) and in the long term (e.g., during development and skill acquisition), and it changes in response to trauma and disease (Capaday 1997; Capaday and Stein 1986; Thompson and Wolpaw 2014; Wolpaw 2006, 2010; Wolpaw and Tennissen 2001).

The corticospinal tract (CST), which originates mainly in sensorimotor cortex (SMC), plays a central role in adjusting the H-reflex pathway to serve the many different behaviors that are implemented by the spinal cord (Chen and Wolpaw 2002; Chen et al. 2002a, 2002b, 2006a, 2006b). We are seeking to define the SMC activation patterns responsible for short-term and long-term control of the H-reflex pathway. Understanding this interaction could lead to new techniques for inducing, guiding, and evaluating recovery after injury and could provide new insight into the acquisition and maintenance of motor skills (Thompson et al. 2013; Thompson and Wolpaw 2014; Wolpaw 2010).

Electrocorticographic (ECoG) recording from the cortical surface is a sensitive measure of activity in the underlying cortex. ECoG recording has greater topographical resolution and spectral range than electroencephalographic (EEG) recording from the scalp and, at the same time, can provide more extensive coverage and possibly greater long-term stability than intracortical microelectrode recording. Many studies have demonstrated correlations between specific ECoG frequency bands at specific locations and actual or imagined movements (e.g., Hermes et al. 2011; Miller et al. 2007, 2010; Pfurtscheller et al. 2003; Pistohl et al. 2008). These results have generated intense interest in the possibilities for using ECoG signals in brain-computer interfaces (BCIs) that can enable people paralyzed by disorders such as amyotrophic lateral sclerosis or high-level spinal cord injury to control robotic arms or other devices (Fifer et al. 2012; Schalk 2010; Schalk and Leuthardt 2011; Yanagisawa et al. 2011).

Present address for reprint requests and other correspondence: C. B. Boulay, The Ottawa Hospital Research Institute, WS124 725 Parkdale Ave., Ottawa, Ontario, K1Y 4E9, Canada (e-mail: cboulay@uottawa.ca).

The present study examined the short-term relationships of SMC ECoG activity with several measures of neurophysiological function. We found that ongoing soleus electromyographic (EMG) activity was related to concurrent SMC ECoG activity and that the soleus H-reflex and associated somatosensory evoked potentials (SEPs) over the SMC were related to prestimulus SMC ECoG activity. The data analysis sought to determine the extent to which ECoG activity predicts soleus EMG activity, H-reflex size, and SEP size. The results reveal a striking difference between the relationship of SMC ECoG to soleus EMG and its relationship to H-reflex size, suggest the mechanisms responsible for short-term cortical control of the H-reflex pathway, and provide new insights into cortical control of motor function and into how that control might be put to clinical use.

MATERIALS AND METHODS

The subjects of the present study were 40 young adult male Sprague-Dawley rats (<5 mo old, weight range 370–660 g at the beginning of the study). All procedures satisfied the *Guide for the Care and Use of Laboratory Animals* (Institute for Laboratory Animal Research, 2010) and had been reviewed and approved by the Institutional Animal Care and Use Committee of the Wadsworth Center.

Implantation of Chronic Recording and Stimulating Electrodes

Under general anesthesia [pentobarbital sodium (60 mg/kg), administered intraperitoneally], each rat was implanted with recording electrodes in the right soleus muscle and over the left (i.e., contralateral) SMC and stimulating electrodes on the right posterior tibial nerve. To place the electrodes over the cortex, the rat was placed in a stereotaxic frame with its head leveled and secured by ear bars and a tooth holder (Chen et al. 2007). A recording electrode (a blunt stainless steel screw, diameter: 0.5 mm) was implanted in the skull just above the dura over the putative hindlimb area of the left SMC, 1.0 mm caudal to the bregma and 2.8 mm lateral to the midline (Paxinos and Watson 2007). The first six rats had a reference electrode placed 2–3 mm posterior to the first electrode. In the subsequent 34 rats, a reference electrode was implanted in the skull over the right olfactory bulb. Nineteen of these thirty-four rats also had an additional recording electrode over the left posterior cortex (3.0 mm distal to the bregma and 2.8 mm lateral to the midline) and another over the hindlimb area of the right SMC (1.0 mm caudal to the bregma and 2.8 mm lateral to the midline).

To elicit the right soleus H-reflex, the posterior tibial nerve was encircled just above the triceps surae branches with a silicone rubber nerve cuff containing a pair of multistranded stainless steel fine wire electrodes. To record soleus EMG activity, the soleus muscle was implanted with a pair of multistranded stainless steel fine wire EMG recording electrodes with the final 0.5 cm stripped. The Teflon-coated wires from the EMG, nerve cuff, and SMC electrodes passed subcutaneously to a connector plug secured on the skull with stainless steel screws and dental cement.

Immediately after surgery, the rat was placed under a heating lamp and given an analgesic [Demerol (0.2 mg), administered intramuscularly]. Once awake, the rat received a second dose of analgesic and was returned to its cage and provided with food and water *ad libitum*. Body weight was measured daily, and a high-calorie dietary supplement [Nutri-Cal (2–4 ml/day), administered *per os*] was given until body weight regained its presurgery level (i.e., typically 3–7 days). Each rat also received a piece of apple (~10 g) every day throughout the study.

ECoG, EMG, H-Reflex, and SEP Measurements

Data collection began at least 10 days after the rat had fully recovered from surgery and the H-reflex had stabilized. Data from the subsequent 10 days were used in this study. During this period, each rat lived in a standard rat cage with a 40-cm flexible cable attached to the skull plug. The cable, which allowed the rat to move freely about the cage, carried the wires from the head-mounted connector plug to an electrical commutator above the cage and from there to bipolar amplifiers (A-M Systems, Carlsborg, WA) and a stimulus isolation unit. For the EMG channel, the amplifier gain was 1,000 and the bandwidth was 100–1,000 Hz. For the one to three ECoG channels, the gain was 10,000 and the bandwidth was 0.1–10,000 Hz. All rats had free access to food and water. Animal well-being was carefully checked several times each day, and body weight was measured weekly. Laboratory lights were dimmed from 2100 to 0600 hours each day.

Stimulus delivery and data collection were under the control of a computer system that monitored ongoing soleus EMG (sampled at 5,000 Hz) continuously 24 h/day everyday for the entire period of the study. Whenever the full wave rectified value of background (i.e., ongoing) EMG from the right soleus muscle remained within a defined range (typically 1–2% of maximum voluntary contraction) for a randomly varying 2.3- to 2.7-s period, the computer initiated an H-reflex/SEP trial. The background EMG requirement ensured that the H-reflex was elicited during maintenance of a specific level of steady-state soleus EMG activity; the rat was usually crouching or standing. In each trial, the computer digitized (at 5,000 Hz) the most recent 500 ms of EMG and ECoG activity, delivered a monophasic stimulus pulse to the nerve cuff, and stored the EMG and ECoG for the 100 ms after the stimulus.¹ Prestimulus data and data more than 30 ms after the stimulus were downsampled to 500 Hz before storage.

Stimulus pulse amplitude and duration were initially set to produce a maximum soleus H-reflex (as well as an M-wave that was typically just above threshold). Pulse duration (usually 0.5 ms) remained fixed. Pulse amplitude was adjusted by the computer after each trial to maintain the soleus M-wave [i.e., average value of full wave rectified EMG in the M-wave interval (typically 2.0–4.0 ms after stimulation)] unchanged throughout data collection. This ensured that the effective strength of the nerve stimulus was stable throughout the experiment despite any changes that occurred in nerve cuff electrode impedance or in other factors (Chen and Wolpaw 1995; Wolpaw 1987). In the course of its normal activity, the animal usually satisfied the background EMG requirement, and thus received nerve cuff stimulation, 2,500–4,500 times/day.

Data Analysis

As noted above, we analyzed 10 consecutive days of data (i.e., 16,000–74,000 trials) from each rat. Data were stored with a custom software package (Elizan III). All offline signal processing, regression analyses, and statistical analyses were performed with custom programs in the Python programming language. Trials were excluded if their data values were consistently flat or dominated by 60-Hz powerline noise. Trials were also excluded due to extreme values in the calculated variables as defined below. After these criteria were applied, we retained 88% of trials.

Variables. For each trial, 500 ms of prestimulus ECoG activity were converted to the frequency domain using a multitaper spectral estimation. Amplitude at each frequency was converted to power by taking 20 times the logarithm (base 10) of the amplitude and then

¹ The 5,000-Hz digitization rate left open the possibility that the ECoG channels (bandwidth 0.1–10,000 Hz) contained aliased high-frequency (2,500–10,000 Hz) activity. However, mammalian ECoG spectral power above 300 Hz is typically below the amplifier noise floor (e.g., Miller et al., 2007b); and thus it would not have affected our results.

centering and scaling the result by the SD. Trials where spectral power was >5 SD away from its mean were excluded.

Principal component analysis of the standardized ECoG spectral power revealed that the first three components were each dominated by one frequency band and that these bands were very similar across rats. Figure 1 shows this striking finding. It indicated that ECoG activity could be represented by the power values for three frequency bands: $\mu\beta$ (5–30 Hz), low γ (γ_1 ; 40–85 Hz), and high γ (γ_2 ; 100–200 Hz). Thus, the powers in these three frequency bands were used as the three ECoG variables. We assessed the correlations of soleus background (i.e., ongoing) EMG amplitude (BGE), soleus H-reflex size, and SEP size with each of these bands.

BGE was calculated as average rectified EMG amplitude during the final 200 ms digitized before nerve stimulation. Trials were excluded if BGE was $>200 \mu\text{V}$ ($\sim 1\%$ of trials). M-wave size was calculated as average rectified EMG amplitude in the M-wave interval (typically 2.0–4.0 ms after nerve stimulation). Trials were excluded if M-wave size was $>400 \mu\text{V}$ ($\sim 1\%$ of trials). H-reflex size was calculated as the average rectified EMG amplitude in the H-reflex interval (typically 6.0–10.0 ms after nerve stimulation). Trials were excluded if H-reflex size was $>700 \mu\text{V}$ ($\sim 2\%$ of trials). Typically, each rat's BGE, M-wave size, and H-reflex size distributions were unimodal with a very lengthy tail at the upper end. The exclusion criteria were selected to exclude this tail.

The SEP over SMC after nerve stimulation is characterized by two pairs of biphasic peaks (i.e., P1-N1 and P2-N2) (Angel and Lemon 1975; Misiaszek and Brooke 2001; Nelson et al. 2001). We examined SEPs in 34 animals with the reference electrode over the olfactory bulb. Of these 34 animals, we excluded 3 animals because the stimulus artifact persisted more than 5 ms and 6 animals because the SEP peak-to-peak amplitude was smaller than 2% of the noise, leaving 25 animals. For these 25 animals, we calculated peak amplitude as the average amplitude in the peak period. Peak periods were determined by visual inspection of the average SEP for each animal (i.e., typical values: P1, 7–10 ms; N1, 11–18 ms; and N2, 30–40 ms). SEP size was calculated as the voltage difference between P1 and N2. No trials were excluded based on SEP size.

Correlations of SMC ECoG with measures of motor and sensory function. The primary goal of the present study was to determine the correlations of SMC activity, measured as ECoG spectral band power, with soleus BGE, H-reflex size, and SMC SEP size. To focus on this correlation, we used multiple linear regression with BGE amplitude, H-reflex size, and SEP each as a dependent variable and the three ECoG band powers identified above in the set of independent variables.

SMC ECoG activity, BGE, H-reflex size, and SEP size are influenced by common sources and by each other. There are diurnal

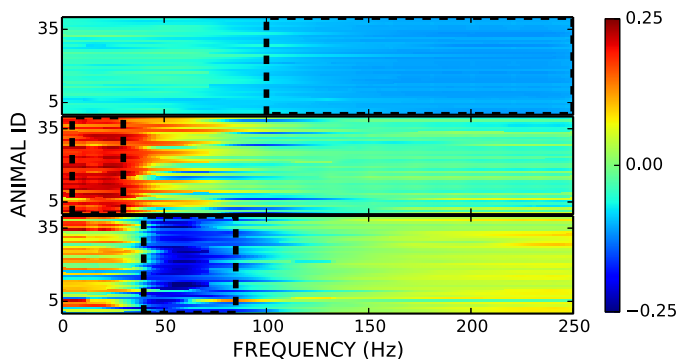


Fig. 1. Principal component (PC) analysis of electrocorticographic (ECoG) spectral power for all rats. The first three components were consistent across the 40 rats (y-axis). The weights for these first three components from 1 to 250 Hz (2-Hz resolution) are shown in arbitrary units ranging from -0.25 to $+0.25$. Bandwidths used for $\mu\beta$ (PC2; middle), γ_1 (PC3; bottom), and γ_2 (PC1; top) are outlined in black dashed lines.

rhythms in ECoG power spectra (Grasing and Szeto 1992), H-reflex size (Chen and Wolpaw 1994; Dowman and Wolpaw 1989), and SEP size (Dowman and Wolpaw 1989). BGE reflects the excitability of spinal cord motor neurons, which covaries with H-reflex size (Capaday and Stein 1986; Larsen and Voigt 2004) and SMC activity (Fetz et al. 1976; Salenius and Hari 2003). H-reflex size varies with stimulus intensity (Capaday 1997). It is important to include these confounding relationships in the model to reveal the independent influence of ECoG on dependent variables. Time of day and stimulus amplitude have nonlinear relationships with dependent variables; thus, we transformed them to linearize their relationships before including them in the linear model.

We calculated the magnitude of the contribution of ECoG power to the estimation of each dependent variables (centered and standardized BGE, H-reflex size, or SEP size) by first calculating R^2 using a multiple-linear regression including all three ECoG bands and all known covariates as independent variables, calculating null- R^2 as the mean of 1,000 R^2 values each obtained after shuffling the trial label for ECoG power independent variables, and then taking the difference of R^2 and null- R^2 . We then calculated the probability that the change in R^2 was greater than zero across animals using one-sample t -tests. We also report the regression coefficients from the unshuffled multiple regressions for each ECoG band and the probability that each regression coefficient is nonzero across animals using one-sample t -tests.

To facilitate visual examination of the effects of prestimulus ECoG power on H-reflex size and SEP size and on linear regressions between BGE and H-reflex size, we averaged separately trials with low prestimulus ECoG power (z -score power < -1) and those with high prestimulus ECoG power (z -score power > 1). We tested for an effect of band power on each measure using paired sample t -tests.

Multichannel ECoG data. In 19 rats, ECoG was recorded from multiple electrodes over the SMC, all referenced to the electrode over the olfactory bulb. For these rats, we performed repeated-measures ANOVAs examining the influence of electrode location on the variance in BGE and H-reflex size accounted for by ECoG power for each ECoG spectral band. Of the 25 rats used in the single-channel SEP analysis, 14 had multichannel ECoG data. In these 14 animals, we examined the influence of electrode location on SEP size.

RESULTS

SMC ECoG Correlates With BGE

As shown in Fig. 2, both ECoG power and BGE magnitude have diurnal rhythms. Thus, we included time of day as a covariate before measuring ECoG correlations with BGE. The full model, including time of day and the three ECoG bands as independent variables, accounted for 5.13% (± 0.60 SE) of the variance in BGE size. The variance accounted for by ECoG was 3.61% (± 0.46) more than expected by chance ($P < 0.001$). The direction of influence of ECoG bands on BGE was frequency dependent. As shown in Fig. 3, BGE correlated negatively with low-frequency ECoG ($\mu\beta$; regression coefficient $b = -0.134 \pm 0.016$, $P < 0.001$) and positively with high-frequency ECoG (γ_1 ; $b = 0.088 \pm 0.015$, $P < 0.001$). Very-high-frequency ECoG did not correlate significantly with BGE (γ_2 ; $b = 0.0223 \pm 0.014$, $P = 0.12$).

SMC ECoG Correlates With H-reflex size When the Effect of BGE Is Removed

Correlations between SMC ECoG activity and H-reflex size are distorted by their diurnal rhythms, and H-reflex size is related to the intensity of the stimulus; therefore, time of day

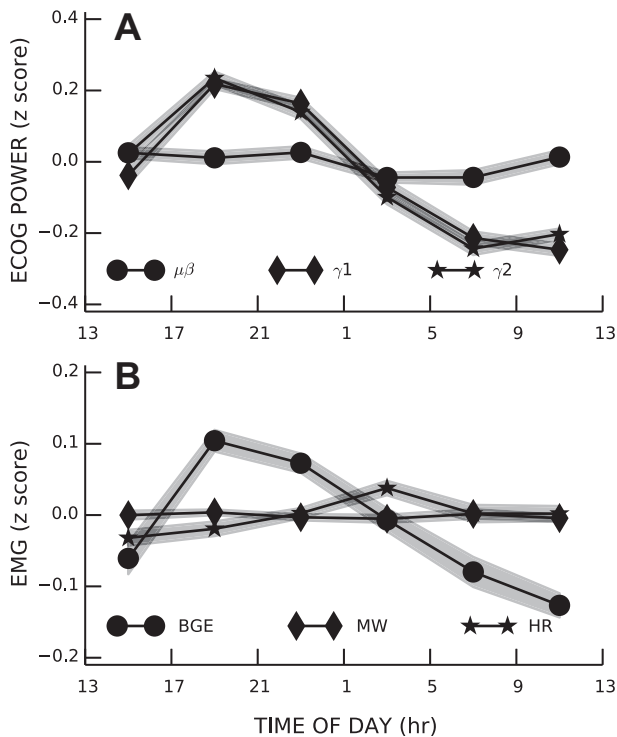


Fig. 2. Diurnal rhythms in the three bands of sensorimotor cortex (SMC) ECoG activity (A) and in soleus background electromyographic (EMG) amplitude (BGE), M-wave (MW), and H-reflex size (HR size; B). Shaded areas represent group SEs.

and stimulus intensity were included as covariates in all subsequent correlations. We first examined correlations between SMC ECoG and H-reflex size. The model, with the set of independent variables comprising stimulus intensity, time of day, and SMC ECoG in three bands, accounted for 2.75% (± 0.54) of the variance in H-reflex size, and the variance accounted for by ECoG was 0.41% (± 0.09) more than expected by chance ($P < 0.001$). H-reflex size is linearly related to BGE (Capaday and Stein 1986; Larsen and Voigt 2004); therefore, we might expect ECoG correlations with H-reflex size to be a transitive property of the relations between ECoG and BGE and between BGE and HR. However, as shown in Fig. 3B (open bars), ECoG band power did not consistently influence H-reflex size ($\mu\beta$; $b = -0.009 \pm 0.009$, $P = 0.341$; $\gamma 1$: $b = 0.008 \pm 0.005$, $P = 0.170$; and $\gamma 2$: $b = 0.010 \pm 0.006$, $P = 0.110$). These results imply that the influence of ECoG power on H-reflex size is not mediated entirely through the influence of ECoG power on BGE.

We then calculated the correlations between ECoG and H-reflex size with BGE added to the covariates. The full model accounted for 13.46% (± 0.83) of the variance in H-reflex size, and the variance accounted for by ECoG was 0.43% (± 0.07) greater than expected by chance ($P < 0.001$). As shown in Fig. 3B (shaded bars), SMC ECoG correlated with HR in a frequency-dependent manner that was opposite to that of BGE (Fig. 3A), that is, the $\mu\beta$ band correlated positively ($b = 0.040 \pm 0.008$, $P < < 0.001$) and the $\gamma 1$ band correlated negatively ($b = -0.028 \pm 0.005$, $P < < 0.001$) with HR (Fig. 3B, shaded bars). ECoG power in the $\gamma 2$ band did not correlate with H-reflex size ($b = 0.000 \pm 0.005$, $P = 0.913$). In summary, when we did not include BGE as a covariate, the correlations

between ECoG and H-reflex size were concealed by the opposing correlations between BGE and ECoG.

H-reflexes elicited by stimuli near the M-wave threshold vary widely in size; thus, the proportion of the variance in H-reflex size accounted for by ECoG is small, despite being highly significant. To visualize the magnitude of the impact of ECoG on H-reflex size, we compared average H-reflex sizes for trials with low $\mu\beta$, $\gamma 1$, or $\gamma 2$ band power to those for trials with high power. Figure 4 shows the results for a representative rat. $\mu\beta$ power had a substantial effect on H-reflex size (up to a 45% change in H-reflex size, mean: 9.1%, $P < 0.001$), whereas $\gamma 1$ power had a small effect (mean: -2.6% , $P = 0.02$) and $\gamma 2$ power had no significant effect (mean: -1.8% , $P = 0.1$).

Changes in H-reflex size can also be described in terms of the changes in the parameters of its linear regression with BGE (Capaday and Stein 1986). For each ECoG band ($\mu\beta$, $\gamma 1$, and $\gamma 2$), we regressed H-reflex size with BGE separately for trials with low band power and trials with high band power, as described above. Figure 5A shows a representative pair of regressions for one rat for low and high $\mu\beta$ power; Fig. 5B shows the group results. The y-intercept parameter of the linear regression was larger with high $\mu\beta$ power [change in y-intercept (in SD units) = 0.09 ± 0.02 , $P < 0.001$] and smaller with high $\gamma 1$ power (-0.03 ± 0.01 , $P = 0.01$) and did not change

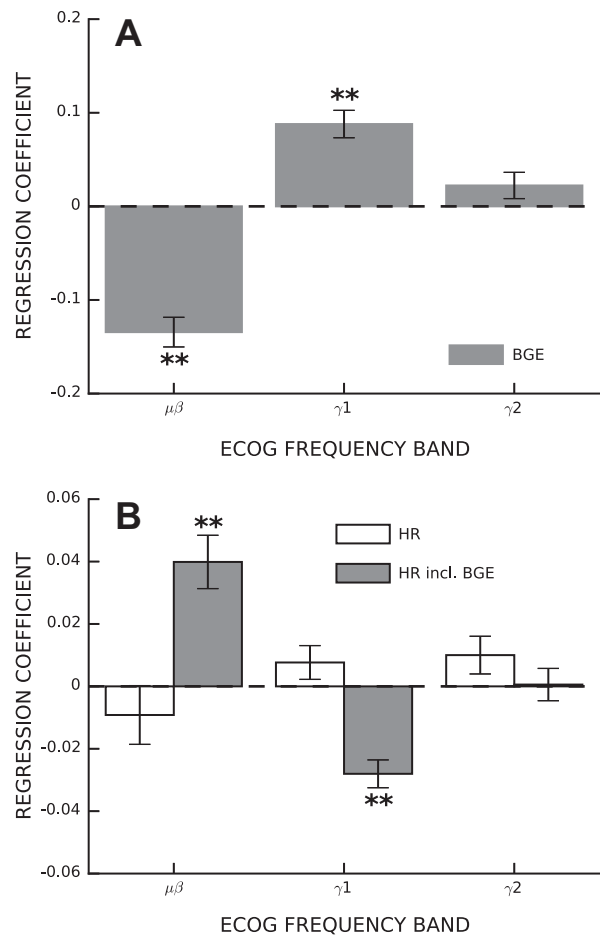


Fig. 3. ECoG activity correlates with BGE and HR size. A: average regression coefficients between ECoG band power and BGE (\pm SE). B: average regression coefficients between ECoG band power and the H-reflex with (solid bars) and without (open bars) BGE included in the list of independent variables. * $P < 0.05$; ** $P < 0.001$.

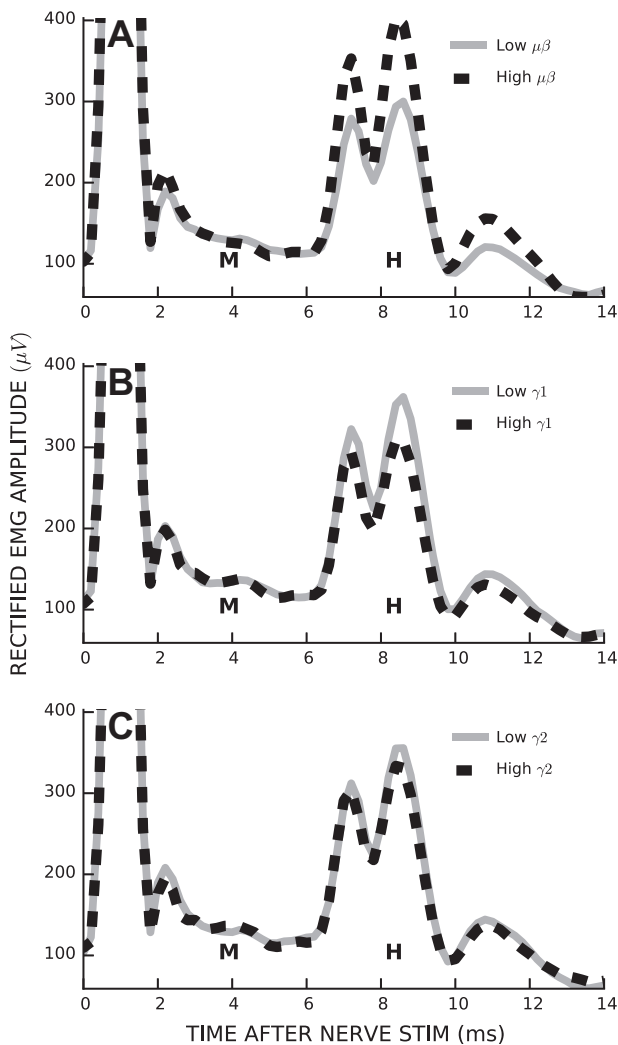


Fig. 4. Stimulus-evoked soleus EMG activity from a representative rat under conditions of low (solid line) and high (dashed line) ECoG band power in $\mu\beta$ (A), γ_1 (B), and γ_2 (C) bands. M, M-wave; H, H-reflex.

with γ_2 power. In contrast, the slope parameter of the linear regression was not affected by power in any of the three bands.

SMC ECoG Correlates Weakly With SEP Size

The stimulus that evoked the H-reflex also evoked a SEP in the ECoG recording. For the 25 rats with SEPs and the ECoG reference electrode over the olfactory bulb (i.e., a putatively inactive reference), we examined the impact of prestimulus ECoG band power on individual peak sizes and SEP size (i.e., P1-N2). Average SEPs for conditions of high and low $\mu\beta$ power from a representative rat are shown in Fig. 6A. The difference in SEP size between high- and low-band powers was significant for the $\mu\beta$ band only ($P = 0.006$). We regressed SEP sizes against the set of independent variables comprising time of day, stimulus intensity, and power in three ECoG bands. The results are shown in Fig. 6B. The full model accounted for 1.00% (± 0.28) of the variance in SEP size, and ECoG power accounted for 0.27% (± 0.07) more of the variance than expected by chance ($P = 0.001$). The correlations between ECoG and SEP size were similar to those between ECoG and H-reflex size (i.e.,

low-frequency activity was associated with larger SEPs and high-frequency activity was associated with smaller SEPs). However, the strengths of the correlations were much weaker for the SEP than for H-reflex size (i.e., $\mu\beta$: $b = 0.025 \pm 0.006$, $P = 0.001$; γ_1 : $b = -0.013 \pm 0.004$, $P = 0.006$; and γ_2 : $b = -0.010 \pm 0.005$, $P = 0.047$).

Topographic Specificity of SMC ECoG Correlations

In addition to the electrode located over the left hindlimb area of the SMC (i.e., contralateral to the soleus muscle from which BGE and the H-reflex were recorded), data were recorded simultaneously from an electrode located 2 mm more posterior and from an electrode over the right hindlimb area of the SMC (i.e., ipsilateral to the recorded muscle) in 19 animals (each referenced to the electrode over the olfactory bulb).

We performed ANOVA on SEP size for the 14 animals with both SEPs and multichannel ECoG data. There was a significant main effect of electrode location [$F(2,11) = 13.62$, $P < 0.001$]. Post hoc pairwise comparisons revealed that the SEP recorded over the left SMC was significantly larger than SEPs recorded over the posterior cortex or right SMC ($P < 0.05$ by Tukey honest significant difference test; Fig. 7A). We performed ANOVA on ECoG band power regression coefficients for both BGE and H-reflex size, including the 19 animals with multichannel ECoG data. There was no main effect of electrode location for regression coefficients of either BGE or H-reflex size for any of the ECoG bands [BGE: $\mu\beta$, $F(2,16) = 0.31$, $P = 0.73$; γ_1 , 0.27 and 0.76; and γ_2 , 0.06 and 0.94; H-reflex size: $\mu\beta$, 0.21 and 0.81; γ_1 , 0.81 and 0.45; and γ_2 , 0.05 and 0.95; Fig. 7B].

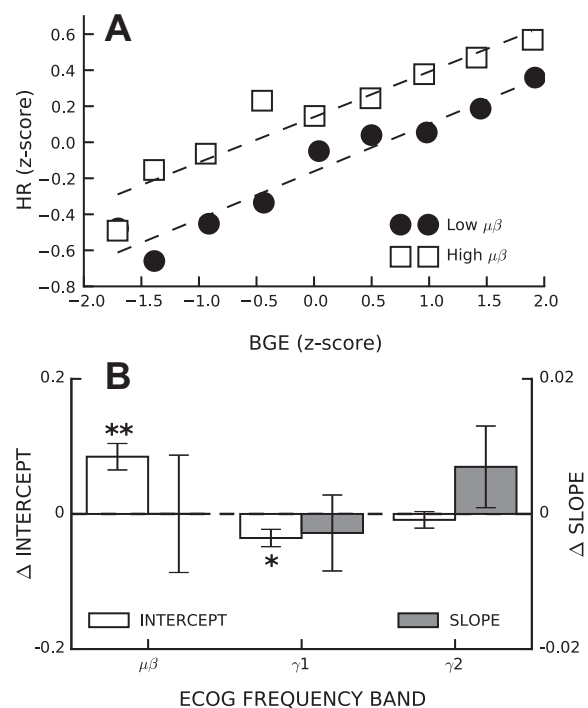


Fig. 5. Changes in SMC ECoG activity affected the intercept but not the slope of the linear relationship between HR size and BGE. A: linear regressions between HR size and ongoing EMG in one rat for trials with low $\mu\beta$ band power (solid circles) and high $\mu\beta$ band power (open squares). B: average (\pm SE) change in intercept (open bars) and slope (closed bars) for linear regressions of HR size versus BGE between conditions of low and high band powers across all rats. * $P < 0.05$; ** $P < 0.001$.

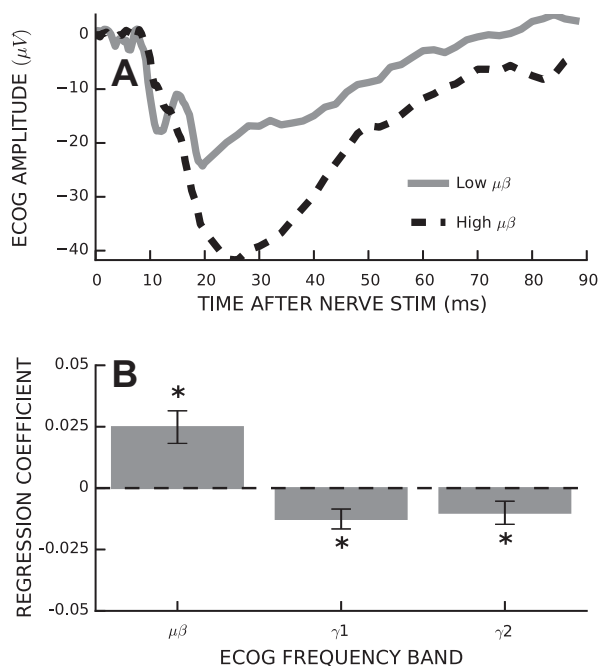


Fig. 6. Prestimulus ECoG power affects somatosensory evoked potential (SEP) size. *A*: average SEPs for a representative rat for trials with low (solid) and high (dashed) $\mu\beta$ band power. *B*: average (\pm SE) regression coefficients relating SEP peak-to-peak size to ECoG band power with time of day and stimulus intensity included in the model. * $P < 0.05$.

DISCUSSION

The present study measured ongoing activity in two CNS areas: SMC (measured as ECoG) and the soleus spinal motor nucleus (measured as soleus EMG). It also measured the response of each area to stimulation of group 1 afferent axons in the posterior tibial nerve (i.e., measured as the SMC SEP and soleus H-reflex, respectively). The primary goal was to determine the impact of SMC activity on H-reflex size, that is, to determine how the SMC affects the simplest motor behavior, the largely monosynaptic motoneuron response to a well-defined sensory input. To do this, we assessed the correlation of SMC activity with ongoing soleus activity before H-reflex elicitation and separated the impact of SMC activity on the H-reflex from that of the ongoing soleus activity. In addition, to compare the impact of SMC activity on the H-reflex with its impact on other components of the CNS response to the sensory input, we assessed the impact of SMC activity on the SMC evoked potential.

SMC ECoG, Soleus EMG, and the Soleus H-Reflex

In general, high-frequency [i.e., γ_1 (40–85 Hz) and γ_2 (100–200 Hz)] ECoG activity is associated with movement or movement imagery and reflects an activated cortical state, whereas low-frequency [i.e., $\mu\beta$ (5–30 Hz)] ECoG is associated with relaxation and reflects an idling or inactivated cortical state (Jerbi et al. 2009; Pfurtscheller et al. 1996; Ray et al. 2008). Our data have similar associations: γ_1 and γ_2 ECoG was higher at night when rats were more active and lower during the day when they were less active. Furthermore, γ_1 ECoG was positively correlated and $\mu\beta$ ECoG was negatively correlated with ongoing soleus EMG. Thus, an activated SMC state was associated with increased soleus activation.

The effect of BGE on H-reflex size is well known: in general, the more active a muscle is, the larger its response to a given excitatory input (at least until BGE approaches its maximum) (Schieppati 1987). If the relation between SMC activation and H-reflex size is merely a transitive property of the relations between SMC and BGE and between BGE and H-reflex size, then we would expect ECoG correlations with H-reflex size to be similar to ECoG correlations with BGE. However, even though ECoG did contribute significantly to H-reflex size estimation, the influence of individual ECoG bands on H-reflex size was not consistent with its effect on BGE. This suggested SMC effect on the H-reflex circuit is not mediated entirely through modulation of ongoing EMG activity.

We assessed this possibility by removing the influence of BGE on H-reflex size. The result was clear: when BGE was included in the model, $\mu\beta$ ECoG was positively correlated and γ_1 ECoG was negatively correlated with H-reflex size. Thus, it appears that SMC has two opposing effects on the H-reflex. The first effect is clearly secondary to the effect of SMC ECoG activity on BGE: an activated SMC state increases the H-reflex because it increases BGE. The second effect is in the opposite direction: an activated SMC state decreases the H-reflex by another mechanism.

Mechanisms and Magnitudes of the Two SMC Effects on H-Reflex Size

The monosynaptic pathway that is largely responsible for the H-reflex is susceptible to influence mainly at two places: presynaptically at the terminal of the primary afferent neuron

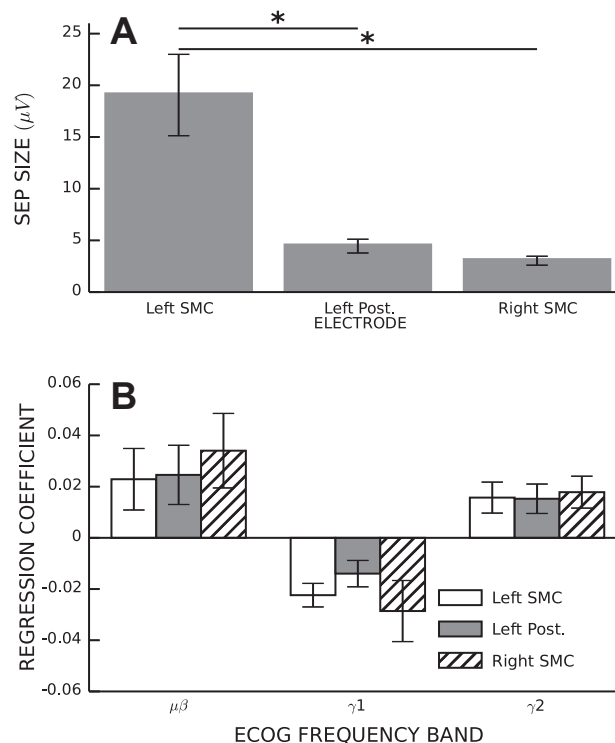


Fig. 7. Topographic specificity of ECoG correlations with HR size and SEP size. *A*: average SEP size (\pm SE) as a function of electrode location. *Significant difference by Tukey honestly significant difference post hoc test ($P < 0.05$). *B*: average regression coefficients (\pm SE) relating ECoG band power to HR size as a function of electrode location.

and postsynaptically at the α -motoneuron (Knikou 2008). The impact of BGE is a postsynaptic effect: H-reflex size increases when the motoneurons are more active and thus more likely to fire in response to afferent input. The mechanism for the second, and opposing, effect associated with SMC ECoG is yet unclear. It is unlikely that SMC state affects motoneuron recruitment gain; it is more likely that the SMC state affects the reliability of transmission at the Ia afferent terminal. This hypothesis is supported by the fact that the SMC state affected the intercept but not the slope of the linear regression between H-reflex size and BGE (Fig. 6). A change in presynaptic inhibition, e.g., might produce an effect of this kind on the regression (Capaday and Stein 1986).

Direct stimulation of the motor cortex decreases presynaptic inhibition of the H-reflex during quiet standing in both cats (Rudomín et al. 1983) and humans (Meunier and Pierrot-Deseilligny 1998; Petersen et al. 1998). In contrast, the present rat study suggests that an activated SMC state (i.e., decreased $\mu\beta$ and increased $\gamma 1$) was associated with increased presynaptic inhibition. This contrast could reflect a difference between the cortical output produced by direct SMC stimulation and that associated with intrinsic SMC activation and/or an interspecies difference in the muscle activation pattern underlying quiet standing.

H-reflex size can be affected by many factors, including motoneuron excitability, time of day, stimulus intensity, limb movement-related changes in nerve-cuff or EMG electrode function, contraction of other muscles (e.g., a Jendrassik maneuver), and probably other unknown influences. As a result, the variance in H-reflex size is very high, and the H-reflex variance accounted for by the SMC state, while statistically significant ($P < 0.001$), is $\leq 1.7\%$ of the total variance (depending on the rat). Nevertheless, the SMC state (as reflected in low- and high-frequency ECoG components) has a substantial impact, as shown in Fig. 4.

Furthermore, the present results may underestimate the impact of SMC on H-reflex size because the relatively large (i.e., 0.5-mm diameter) and epidural ECoG electrodes probably lacked sufficient spatial resolution to target the specific cortical neural assemblies directly responsible for soleus H-reflex modulation. Thus, they are likely to reflect widespread SMC activation rather than activation of a relatively small area. This speculation is supported by the weak topographical specificity of the correlations between the SMC state and H-reflex size and between SMC state and BGE. High-resolution ECoG devices (Kim et al. 2007; Thongpang et al. 2011) or intracortical microelectrodes (Campbell et al. 2002), which could provide much better spatial resolution, might reveal much stronger correlations between the SMC state and H-reflex size.

SMC ECoG and the SEP

In addition to its impact on H-reflex size, the SMC state also affected the amplitude of the SEP produced by the stimulus that elicited the H-reflex. This effect was similar to, though weaker than, that on the H-reflex; SEP size correlated positively with power in low-frequency ($\mu\beta$) ECoG and negatively with power in high-frequency ($\gamma 1$) ECoG. Since the pathway that produces the SEP does not include the primary afferent synapse on the spinal motoneuron or the motoneuron itself, this SEP effect was presumably produced elsewhere. Studies in

which EPs are recorded at each stage in the ascending pathways could help to determine the site of SEP modulation.

Alternatively or in addition, SEP size modulation could reflect the impact of the SMC state on cortical processing. A related possibility is also worth considering. Although ongoing cortical electrical activity is traditionally viewed as noise on which SEPs are simply superimposed, recent evidence suggests that SEP components may represent synchronization of ongoing cortical oscillations (Fellinger et al. 2011; Makeig et al. 2002; Sauseng et al. 2007). If SEP size reflects synchronization of low-frequency ($\mu\beta$) ECoG activity, its positive correlation with $\mu\beta$ power might be expected.

SMC Influence on H-Reflex Size and Motor Function

Even when ongoing muscle activity does not change, H-reflex size can change as a function of the current motor behavior. For example, soleus H-reflexes are larger during walking than during running and larger during standing than during walking, even when BGE is the same (Capaday and Stein 1986, 1987; Edamura et al. 1991; Simonsen and Dyhre-Poulsen 1999; Stein 1995). Furthermore, the relationship between H-reflex size and BGE changes over the course of the normal step cycle (Capaday and Stein 1986; Knikou et al. 2009). These changes in H-reflex size are believed to reflect changes in presynaptic inhibition at the primary afferent synapse on the motoneuron. They are task-dependent adaptations, changes in H-reflex size that presumably serve the needs of the current task. The ability to make these task-dependent adaptations quickly and appropriately (e.g., changing presynaptic inhibition to suit the current task) is an essential part of the skill of standing, walking, or running. While these quick adaptations do require an intact spinal cord (Phadke et al. 2010), it remains to be determined whether they are produced by changes in the SMC state like those described here.

Thompson et al. (2009) showed that people can learn to produce a task-dependent adaptation (i.e., increase or decrease) in H-reflex size, without a change in BGE, when rewarded for doing so. The ability was acquired over two to six training sessions, in each of which the soleus H-reflex was elicited 225 times and the person was informed each time as to whether the H-reflex met a size criterion. This task-dependent adaptation was clearly differentiated from a long-term change in H-reflex size, which developed gradually over many more sessions. Change in presynaptic inhibition is the most likely mechanism of this task-dependent adaptation, and available evidence from both humans and animals suggests that the SMC is responsible (Segal 1997; Thompson and Wolpaw 2014; Wolpaw and Chen 2009). If further studies find that task-dependent adaptations in H-reflex size do reflect changes in the SMC state, it will be clear that the immediate role of the SMC in motor function goes beyond its well-known direct activation of spinal motoneurons.

At the same time, the relationship between short-term SMC control of H-reflex size described in the present study and the long-term H-reflex change produced by prolonged operant conditioning, which definitely depends on the SMC (Chen et al. 2006a), remains unclear. While the former is probably mediated by presynaptic inhibition, the latter is likely to reflect postsynaptic changes in the motoneuron itself as well as changes elsewhere in the spinal cord (Thompson and Wolpaw

2014; Wolpaw 2010; Wolpaw and Chen 2009), and the extent to which they are independent of each other is not known.

Clinical Implications of the Present Results

Reflex conditioning protocols for rehabilitation. Studies in both animals and humans have suggested that operant conditioning of spinal reflexes can be used to guide plasticity so as to restore more effective motor function to those with partial spinal cord injuries or other neuromuscular disorders (Chen et al. 2006c, 2010; Thompson et al. 2013). Reflex conditioning protocols might conceivably be more effective if they based reward (i.e., positive feedback) in whole or in part on the SMC electrical activity associated with the desired change in reflex size rather than basing it solely on reflex size. Practical clinical use of this strategy would depend on identification of one or more topographically focused scalp-recorded EEG components in μ , β , or low- γ frequency bands that correlate strongly with the size of the targeted reflex.

BCIs for communication and control. The present results are relevant for the development of BCIs that can restore communication and control capacities to those with severe neuromuscular disabilities (Wolpaw and Wolpaw 2012). BCIs might use SMC ECoG to determine the action the BCI user wants to perform and then produce the action (Schalk 2012). This strategy is based on the evidence that SMC ECoG activity is closely correlated with intended movement. However, these correlations are typically documented under highly controlled conditions. It is not clear how well they will generalize to the continually varying real-life conditions in which BCIs need to operate. Indeed, the inconsistent performance typical of current BCIs suggests that the correlations between cortical activity and intention are affected by a variety of as-yet-undefined factors.

The present study shows that a very simple motor function, the soleus H-reflex, correlated with SMC ECoG when soleus EMG was controlled but did not do so when soleus EMG was not controlled. Thus, in a BCI context, SMC ECoG indicates the intended soleus H-reflex gain when soleus EMG is constant (or when soleus EMG is measured and factored out), but it does not do so when soleus EMG varies and is not taken into account. The implication is that the correlations between cortical activity and motor function found under specific conditions do not necessarily generalize to other conditions. Successful translation of BCI systems from the laboratory to the home will require algorithms that can function reliably amid the highly varying cognitive, behavioral, and environmental circumstances of normal life. In addition to providing a simple example of the general problem, the present results show that taking BGE (as an indicator of descending drive to motoneurons) into account may be one way of enhancing BCI reliability.

Conclusions

This study extends understanding of the short-term relationship between the SMC state and motor function. In addition to its well-known role in controlling muscle contraction, the SMC state affects the earliest CNS response to input from muscle spindle receptors: the largely monosynaptic reflex measured here as the H-reflex. When the impact of BGE on H-reflex size is removed, low-frequency SMC ECoG is associated with

larger H-reflexes and high-frequency activity is associated with smaller H-reflexes. These correlations are opposite to those between SMC ECoG activity and BGE level. They may reflect change in presynaptic inhibition at the primary afferent synapse on the motoneuron. The SMC SEP displays correlations with ongoing SMC ECoG similar to those of the H-reflex. These results have implications for the development of new motor rehabilitation methods and for the development of BCIs that rely on correlations between SMC activity and intended motor outputs.

ACKNOWLEDGMENTS

The authors thank Rong-Liang Liu and Lu Chen for excellent technical assistance and Dr. Jonathan S. Carp for valuable advice and comments on the manuscript.

GRANTS

This work was supported by National Institutes of Health Grants NS-22189 (to J. R. Wolpaw), NS-061823 (to X. Y. Chen and J. R. Wolpaw), and HD-36020 (to X. Y. Chen) and by The NYS Spinal Cord Injury Research Board (to X. Y. Chen).

DISCLOSURES

No conflicts of interest, financial or otherwise, are declared by the author(s).

AUTHOR CONTRIBUTIONS

Author contributions: C.B.B. analyzed data; C.B.B. and J.R.W. interpreted results of experiments; C.B.B. prepared figures; C.B.B. drafted manuscript; C.B.B. and J.R.W. edited and revised manuscript; C.B.B. and J.R.W. approved final version of manuscript; X.Y.C. and J.R.W. conception and design of research; X.Y.C. performed experiments.

REFERENCES

- Angel A, Lemon RN. Sensorimotor cortical representation in the rat and the role of the cortex in the production of sensory myoclonic jerks. *J Physiol* 248: 465–488, 1975.
- Ashe J, Lungu OV, Basford AT, Lu X. Cortical control of motor sequences. *Curr Opin Neurobiol* 16: 213–221, 2006.
- Campbell PK, Jones KE, Huber RJ, Horch KW, Normann RA. A silicon-based, three-dimensional neural interface: manufacturing processes for an intracortical electrode array. *IEEE Trans Biomed Eng* 38: 758–768, 2002.
- Capaday C, Stein RB. Amplitude modulation of the soleus H-reflex in the human during walking and standing. *J Neurosci* 6: 1308–1313, 1986.
- Capaday C, Stein RB. Difference in the amplitude of the human soleus H reflex during walking and running. *J Physiol* 392: 513–522, 1987.
- Capaday C. Neurophysiological methods for studies of the motor system in freely moving human subjects. *J Neurosci Methods* 74: 201–218, 1997.
- Chen XY, Carp JS, Chen L, Wolpaw JR. Corticospinal tract transection prevents operantly conditioned H-reflex increase in rats. *Exp Brain Res* 144: 88–94, 2002a.
- Chen XY, Carp JS, Chen L, Wolpaw JR. Sensorimotor cortex ablation prevents H-reflex up-conditioning and causes a paradoxical response to down-conditioning in rats. *J Neurophysiol* 96: 119–27, 2006a.
- Chen XY, Chen L, Wolpaw JR, Jakeman LB. Corticospinal tract transection reduces H-reflex circadian rhythm in rats. *Brain Res* 942: 101–8, 2002b.
- Chen XY, Chen Y, Chen L, Tenissen AM, Wolpaw JR. Corticospinal tract transection permanently abolishes H-reflex down-conditioning in rats. *J Neurotrauma* 23: 1705–1712, 2006b.
- Chen XY, Pillai S, Chen Y, Wang Y, Chen L, Carp JS, Wolpaw JR. Spinal and supraspinal effects of long-term stimulation of sensorimotor cortex in rats. *J Neurophysiol* 98: 878–887, 2007.
- Chen XY, Wolpaw JR. Circadian rhythm in rat H-reflex. *Brain Res* 648: 167–170, 1994.
- Chen XY, Wolpaw JR. Operant conditioning of H-reflex in freely moving rats. *J Neurophysiol* 73: 411–415, 1995.

- Chen XY, Wolpaw JR.** Probable corticospinal tract control of spinal cord plasticity in the rat. *J Neurophysiol* 87: 645–652, 2002.
- Chen Y, Chen XY, Jakeman LB, Chen L, Stokes BT, Wolpaw JR.** Operant conditioning of H-reflex can correct a locomotor abnormality after spinal cord injury in rats. *J Neurosci* 26: 12537–12543, 2006c.
- Chen Y, Wang Y, Chen L, Sun C, English AW, Wolpaw JR, Chen XY.** H-reflex up-conditioning encourages recovery of EMG activity and H-reflexes after sciatic nerve transection and repair in rats. *J Neurosci* 30: 16128–16136, 2010.
- Dowman R, Wolpaw JR.** Diurnal rhythms in primate spinal reflexes and accompanying cortical somatosensory evoked potentials. *Electroencephalogr Clin Neurophysiol* 72: 69–80, 1989.
- Edamura M, Yang JF, Stein RB.** Factors that determine the magnitude and time course of human H-reflexes in locomotion. *J Neurosci* 11: 420–427, 1991.
- Fellinger R, Klimesch W, Gruber W, Freunberger R, Doppelmayr M.** Pre-stimulus alpha phase-alignment predicts P1-amplitude. *Brain Res Bull* 85: 417–423, 2011.
- Ferrier D.** *The Functions of the Brain*. New York: G. P. Putnam's Sons, 1886.
- Fetz EE, Cheney P, German D.** Corticomotoneuronal connections of precentral cells detected by postspike averages of EMG activity in behaving monkeys. *Brain Res* 114: 505–510, 1976.
- Fifer MS, Acharya S, Benz HL, Mollazadeh M, Crone NE, Thakor NV.** Toward electrocorticographic control of a dexterous upper limb prosthesis: building brain-machine interfaces. *IEEE Pulse* 3: 38–42, 2012.
- Fritsch G, Hitzig E.** On the electrical excitability of the cerebrum. *Arch Anat Physiol Wissenschaft Med* 37: 300–332, 1870.
- Grasing K, Szeto H.** Diurnal variation in continuous measures of the rat EEG power spectra. *Physiol Behav* 51: 249–254, 1992.
- Graziano MS, Taylor CSR, Moore T, Cooke DF.** The cortical control of movement revisited. *Neuron* 36: 349–362, 2002.
- Gross CG.** The discovery of motor cortex and its background. *J Hist Neurosci* 16: 320–331, 2007.
- Henneman E, Somjen G, Carpenter DO.** Excitability and inhibibility of motoneurons of different sizes. *J Neurophysiol* 28: 599–620, 1965.
- Hermes D, Miller KJ, Vansteensel MJ, Aarnoutse EJ, Leijten FS, Ramsey NF.** Neurophysiological correlates of fMRI in human motor cortex. *Hum Brain Mapp* 33: 1689–1699, 2011.
- Institute for Laboratory Animal Research.** *Guide for the Care and Use of Laboratory Animals* (8th ed.). Washington, DC: National Academy, 2010.
- Jerbi K, Ossandón T, Hamamé CCM, Senova S, Dalal SS, Jung J, Minotti L, Bertrand O, Berthoz A, Kahane P, Lachaux JP.** Task-related gamma-band dynamics from an intracerebral perspective: review and implications for surface EEG and MEG. *Hum Brain Mapp* 30: 1758–1771, 2009.
- Kim J, Wilson JA, Williams JC.** A cortical recording platform utilizing microECoG electrode arrays. *Conf Proc Annu Int Conf IEEE Eng Med Biol Soc* 2007: 5353–5357, 2007.
- Knikou M, Angeli CA, Ferreira CK, Harkema SJ.** Soleus H-reflex modulation during body weight support treadmill walking in spinal cord intact and injured subjects. *Exp Brain Res* 193: 397–407, 2009.
- Knikou M.** The H-reflex as a probe: pathways and pitfalls. *J Neurosci Methods* 171: 1–12, 2008.
- Larsen B, Voigt M.** Changes in the gain of the soleus H-reflex with changes in the motor recruitment level and/or movement speed. *Eur J Appl Physiol* 93: 19–29, 2004.
- Makeig S, Westerfield M, Jung TP, Enghoff S, Townsend J, Courchesne E, Sejnowski TJ.** Dynamic brain sources of visual evoked responses. *Science* 295: 690–694, 2002.
- Matthews PB.** *Mammalian Muscle Receptors and Their Central Actions*. London: Edward Arnold, 1972.
- Meunier S, Pierrot-Deseilligny E.** Cortical control of presynaptic inhibition of Ia afferents in humans. *Exp Brain Res* 119: 415–426, 1998.
- Miller KJ, Hermes D, Honey CJ, Hebb AO, Ramsey NF, Knight RT, Ojemann JG, Fetz EE.** Human motor cortical activity is selectively phase-entrained on underlying rhythms. *PLoS Comput Biol* 8: e1002655, 2012.
- Miller KJ, Leuthardt EC, Schalk G, Rao RP, Anderson NR, Moran DW, Miller JW, Ojemann JG.** Spectral changes in cortical surface potentials during motor movement. *J Neurosci* 27: 2424–2432, 2007a.
- Miller KJ, Schalk G, Fetz EE, den Nijs M, Ojemann JG, Rao RP.** Cortical activity during motor execution, motor imagery, and imagery-based online feedback. *Proc Natl Acad Sci USA* 107: 4430–4435, 2010.
- Miller KJ, Sorensen LB, Ojemann J.** ECoG observations of power-law scaling in the human cortex. *Arxiv*; <http://arxiv.org/pdf/0712.0846.pdf>, 2007b.
- Misiaszsek JE, Brooke JD.** Vibration-induced inhibition of the early components of the tibial nerve somatosensory evoked potential is mediated at a spinal synapse. *Clin Neurophysiol* 112: 324–329, 2001.
- Nelson AJ, Brooke JD, McIlroy WE, Bishop DC, Norrie RG.** The gain of initial somatosensory evoked potentials alters with practice of an accurate motor task. *Brain Res* 890: 272–279, 2001.
- Paxinos G, Watson C.** *The Rat Brain in Stereotaxic Coordinates*. Oxford: Academic, 2007.
- Petersen N, Christensen LO, Nielsen J.** The effect of transcranial magnetic stimulation on the soleus H reflex during human walking. *J Physiol* 513: 599–610, 1998.
- Pfurtscheller G, Graimann B, Huggins JE, Levine SP, Schuh LA.** Spatio-temporal patterns of beta desynchronization and gamma synchronization in corticographic data during self-paced movement. *Clin Neurophysiol* 114: 1226–1236, 2003.
- Pfurtscheller G, Stancák A, Neuper C.** Event-related synchronization (ERS) in the alpha band—an electrophysiological correlate of cortical idling: a review. *Int J Psychophysiol* 24: 39–46, 1996.
- Phadke CP, Thompson FJ, Kukulka CG, Nair PM, Bowden MG, Madhavan S, Trimble MH, Behrman AL.** Soleus H-reflex modulation after motor incomplete spinal cord injury: effects of body position and walking speed. *J Spinal Cord Med* 33: 371–378, 2010.
- Pistohl T, Ball T, Schulze-Bonhage A, Aertsen A, Mehring C.** Prediction of arm movement trajectories from ECoG-recordings in humans. *J Neurosci Methods* 167: 105–114, 2008.
- Ray S, Niebur E, Hsiao SS, Sinai A, Crone NE.** High-frequency gamma activity (80–150Hz) is increased in human cortex during selective attention. *Clin Neurophysiol* 119: 116–133, 2008.
- Rizzolatti G, Luppino G.** The cortical motor system. *Neuron* 31: 889–901, 2001.
- Rudomín P, Jiménez I, Solodkin M, Dueñas S.** Sites of action of segmental and descending control of transmission on pathways mediating PAD of Ia- and Ib-afferent fibers in cat spinal cord. *J Neurophysiol* 50: 743–769, 1983.
- Salenius S, Hari R.** Synchronous cortical oscillatory activity during motor action. *Curr Opin Neurobiol* 13: 678–684, 2003.
- Sauseng P, Klimesch W, Gruber WR, Hanslmayr S, Freunberger R, Doppelmayr M.** Are event-related potential components generated by phase resetting of brain oscillations? A critical discussion. *Neuroscience* 146: 1435–1444, 2007.
- Schalk G, Leuthardt EC.** Brain computer interfaces using electrocorticographic (ECoG) signals. *IEEE Rev Biomed Eng* 4: 140–154, 2011.
- Schalk G.** Can electrocorticography (ECoG) support robust and powerful brain-computer interfaces? *Front Neuroeng* 3: 9, 2010.
- Schalk G.** BCIs that use electrocorticographic activity. In: *Brain-Computer Interfaces: Principles and Practice*, edited by Wolpaw JR, Wolpaw EW. Oxford: Oxford Univ. Press, 2012, p. 251–264.
- Schieppati M.** The Hoffmann reflex: a means of assessing spinal reflex excitability and its descending control in man. *Prog Neurobiol* 28: 345–376, 1987.
- Segal RL.** Plasticity in the central nervous system: operant conditioning of the spinal stretch reflex. *Top Stroke Rehabil* 3: 76–87, 1997.
- Simonsen EB, Dyhre-Poulsen P.** Amplitude of the human soleus H reflex during walking and running. *J Physiol* 515: 929–939, 1999.
- Stein RB.** Presynaptic inhibition in humans. *Prog Neurobiol* 47: 533–544, 1995.
- Thompson AK, Chen XY, Wolpaw JR.** Acquisition of a simple motor skill: task-dependent adaptation plus long-term change in the human soleus H-reflex. *J Neurosci* 29: 5784–5792, 2009.
- Thompson AK, Pomerantz FR, Wolpaw JR.** Operant conditioning of a spinal reflex can improve locomotion after spinal cord injury in humans. *J Neurosci* 33: 2365–2375, 2013.
- Thompson AK, Wolpaw JR.** Operant conditioning of spinal reflexes: from basic science to clinical therapy. *Front Integr Neurosci* 8: 25, 2014.
- Thongpang S, Richner TJ, Brodnick S, Schendel A, Kim J, Wilson JA, Hippensteel J, LK, Moran DW, Ahmed A, Neimann D, Sillay K, Williams JC.** A micro-electrocorticography platform and deployment strategies for chronic BCI applications. *Clin EEG Neurosci* 42: 259–265, 2011.
- Wolpaw JR, Chen XY.** Operant conditioning of reflexes. In: *Encyclopedia Neuroscience*. Oxford: Academic, 2009, p. 225–233.
- Wolpaw JR, Tennissen AM.** Activity-dependent spinal cord plasticity in health and disease. *Annu Rev Neurosci* 24: 807–843, 2001.

- Wolpaw JR, Wolpaw EW (editors).** *Brain-Computer Interfaces: Principles and Practice*. Oxford: Oxford Univ. Press, 2012.
- Wolpaw JR.** Operant conditioning of primate spinal reflexes: the H-reflex. *J Neurophysiol* 57: 443–459, 1987.
- Wolpaw JR.** The education and re-education of the spinal cord. *Prog Brain Res* 157: 261–280, 2006.
- Wolpaw JR.** What can the spinal cord teach us about learning and memory? *Neuroscience* 16: 532–549, 2010.
- Yanagisawa T, Hirata M, Saitoh Y, Kishima H, Matsushita K, Goto T, Fukuma R, Yokoi H, Kamitani Y, Yoshimine T.** Electrocorticographic control of a prosthetic arm in paralyzed patients. *Ann Neurol* 71: 353–361, 2011.

